AD-A145 808 RESEARCH ON MATERIALS AND COMPONENTS FOR OPTO-ELECTRONIC SIGNAL PROCESSIN..(U) CALIFORNIA UNIV SAN DIEGO LA JOLLA DEPT OF ELECTRICAL ENGINEE.. 1/1

UNCLASSIFIED W S CHANG ET AL. 24 JAN 84 AFOSR-TR-84-0823 F/G 20/12 NL

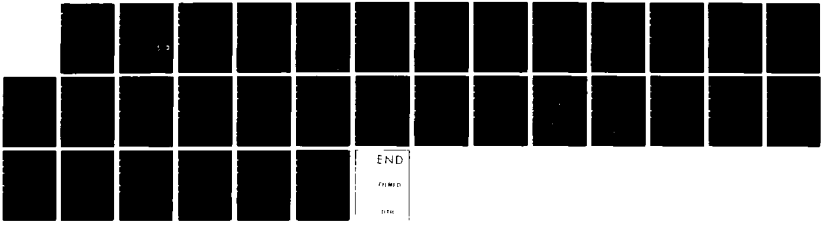

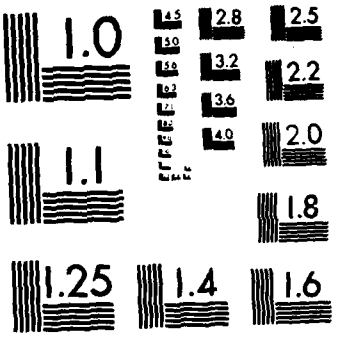

MICROCOPY RESOLUTION TEST CHART
NATIONAL BUREAU OF STANDARDS-1963-A

SECURITY CLASSIFICATION OF THIS PAGE (When Data Entered)

REPORT DOCUMENTATION PAGE

READ INSTRUCTIONS BEFORE COMPLETING FORM

1. REPORT NUMBER: AFOSR-TR- 84 0893
2. GOVT ACCESSION NO.
3. RECIPIENT'S CATALOG NUMBER

4. TITLE (and Subtitle)
Research on Materials and Components for Opto-Electronic Signal Processing

5. TYPE OF REPORT & PERIOD COVERED
Annual Report
10/1/82 - 9/30/83

6. PERFORMING ORG. REPORT NUMBER

7. AUTHOR(s)
William S. C. Chang, Jean-Marc Delavaux, Siamak Forouhar, Timothy Van Eck, L. M. Walpita, Christopher Warren and H. H. Wieder

8. CONTRACT OR GRANT NUMBER(s)
AFOSR-80-0037

PERFORMING ORGANIZATION NAME AND ADDRESS
Dept. of Electrical Engineering & Computer Sciences
University of California, San Diego
La Jolla, CA 92093

10. PROGRAM ELEMENT, PROJECT, TASK AREA & WORK UNIT NUMBERS
61102F 2305 B1

CONTROLLING OFFICE NAME AND ADDRESS
same as block 14

12. REPORT DATE
January 24th, 1984

13. NUMBER OF PAGES
32

14. MONITORING AGENCY NAME & ADDRESS(if different from Controlling Office)
Col. Robert Carter
AFOSR/NE, Bolling Air Force Base
Washington, DC 20332

15. SECURITY CLASS. (of this report)
unclassified

15a. DECLASSIFICATION/DOWNGRADING SCHEDULE

16. DISTRIBUTION STATEMENT (of this Report)

Approved for public release;
distribution unlimited.

17. DISTRIBUTION STATEMENT (of the abstract entered in Block 20, if different from Report)

DTIC
ELECTE
SEP 25 1984
S D
B

18. SUPPLEMENTARY NOTES

19. KEY WORDS (Continue on reverse side if necessary and identify by block number)
fresnel and chirped grating lens, waveguide lens

20. ABSTRACT (Continue on reverse side if necessary and identify by block number)

A number of papers representing the accumulated research results on the chirped grating lenses have been prepared and submitted for publication. They are summarized in this report. A new direction of research to investigate the use of III-V compound semiconductors has shown that very large electro-optical effects may be expected in this wavelength range.

DD FORM 1 JAN 73 1473 EDITION OF 1 NOV 65 IS OBSOLETE

SECURITY CLASSIFICATION OF THIS PAGE (When Data Entered)

INTERIM SCIENTIFIC REPORT

Research on Materials and Components for Opto-Electronic Signal Processing

AFOSR Grant No. 80-0037

October 1st, 1982 through September 30th, 1983

submitted by

William S. C. Chang (Principal Investigator)

Jean-Marc Delavaux, Siamak Forouhar

Timothy Van Eck, L. M. Walpita

Christopher Warren and H. H. Wieder

Department of Electrical Engineering and Computer Sciences

C-014

University of California, San Diego

La Jolla

California 92093

Tel: 619/452-2737

1. Overview

For signal processing in planar waveguides, it is necesary to integrate, focus, collimate, image or Fourier-analyze guided-wave beams by efficient and low cost lenses that have both diffraction-limited performance and low noise. The investigation of chirped grating lenses as shown in Figure 1 has been the principal topic of this research contract until September 1982. Since October 1982 research effort on the $LiNbO_3$ waveguide lens has been shifted partially to a new applied research program awarded jointly to the TRW Technology Research Center and the University of California San Diego (UCSD) in FY83 under the sponsorship of the Air Force Avionics Laboratory, Contract No. F33615-82-C-1751, entitled "Optical Waveguide Diffraction Elements". Only the research concerning the fundamental limitations of the chirped grating lenses has remained in this contract. All the research on lenses will be shifted to the joint TRW-UCSD program in FY84.

In the meantime, a new materials and device research program on the investigation of the electro-optical effects of III-V compound semiconductor materials and devices near their bandgap has been initiated in FY83. We have expected to see a very large electro-optical effect in that wavelength region. Such a large electro-optical effect may lead to high speed guided wave and spatial modulators and signal processors that may eventually have nano seconds of response time. Optical signal processing components may also be interconnected directly with electronic signal processing components in the future in such materials, thereby breaking the current bottleneck that severely restricts the applications of opto-electronic signal processing.

2. Research on Chirped Grating Lenses

A lot of research has been accomplished. Most of the results in the investigation of chirped grating lenses have been or are in the process of being written into papers for publication. Thus, only the titles (and projected titles) and the abstracts (and projected abstracts) are listed below. These papers will be distributed later according to the AFOSR distribution list as soon as reprints are available.

1. A Perturbation and Iterative Perturbation Analysis of Linearly Chirped Grating Lenses of Medium Q in Dielectric Waveguides, by Siamak Forouhar and William S. C. Chang (supported by AFOSR Grant No. 80-0037, accepted for publication in April by the Journal of Quantum Electronics). In this paper a perturbation and iterative perturbation analysis of linearly chirped quasi-periodic structures of medium Q factor in planar dielectric waveguides has been formulated. This analysis can be used to calculate the diffraction efficiency and angular field of view of a given linearly chirped grating structure for a specific incident beam including the effect of higher orders of diffraction. The numerical example of a lens with parameters F = 10, f = 10 mm, Λ_{min} = 2.06 μm, Λ_{max} = 4.25 μm and grating groove length = 15 μm is presented.

2. Performance Limitations of Chirped Grating Lenses on Ti-Indiffused $LiNbO_3$ Planar Waveguides, by Siamak Forouhar, William S. C. Chang (UCSD) and Shih-Kay Yao (TRW) (supported by AFOSR Grant No. 80-0037 and Avionics Laboratory Contract No. F33615-82-C-1751, accepted for publication in the IEEE Journal on Lightwave Technology). In this paper we discuss the design, the fabrication and the experimentally measured performance of the etched and the

deposited chirped grating lenses on Ti-indiffused $LiNbO_3$ waveguides. The materials and fabrication processes developed and the performance limitations imposed by the waveguide parameters and by the fabrication procedures are presented.

3. Chirped Grating Lenses on Nb_2O_5 Transition Waveguides, by Siamak Forouhar, Ron-Xin Lu, William S. C. Chang (UCSD) and Richard L. Davis (Motorola) and Shih-Kay Yao (TRW) (supported by AFOSR Grant No. 80-0037, published in Applied Optics, 22, 3128-1332, 1983). We demonstrate here efficient tapered Nb_2O_5 transition waveguides obtained by reactive sputtering. It provides effective interconnection between two sections of Ti-indiffused waveguide with 0.8 dB total insertion loss. Chirped grating lenses have been fabricated on Nb_2O_5 waveguides that have yielded 85% throughput efficiency. For signal processing applications in Ti-indiffused waveguides, the combination of grating lenses and Nb_2O_5 transition waveguides will allow us to have both high efficiency and large angular field of view.

4. Double Ion Exchanged Chirp Grating Lenses in Lithium Niobate Waveguides, by Christopher Warren, Siamak Forouhar, William S. C. Chang (UCSD) and S. K. Yao (TRW) (supported by AFOSR Grant No. 80-0037, published in Appl. Phys. Lett., Vol. 43, p.424, 1983). In this work, an integrated optical chirped grating lens has been produced which exhibits high throughput efficiency (75%) and large angular field of view (3°). The waveguide substrate is x-cut lithium niobate, and ion exchange in benzoic acid is the method used for making the lens and the waveguide.

5. Effects of Water Vapor on Modes in Ti-Indiffused $LiNbO_3$ Planar Waveguides, by S. Forouhar, G. E. Betts and W. S. C. Chang (supported by AFOSR Grant No. 80-0037 and the General Dynammics Corporation; submitted for publication to Appl. Phys. Lett.). Here, we report two observations concerning the addition of water vapor to the O_2 gas flowing during Ti indiffusion in $LiNbO_3$. 1) Out diffusion is not completely suppressed (e.g. at 1100°C an outdiffused mode occurs after 40 min. when the flowing gas is 85% H_2O). 2) Water vapor has an effect on the indiffused modes that is not due to suppression of outdiffusion. We compare planar guides diffused in dry O_2, wet O_2 and $LiNbO_3$ powder to show this effect. Our data supports the hypothesis that water vapor reduces the Ti diffusion constant.

6. C_2F_6 Reactive Ion Beam Etching of $LiNbO_3$ and Nb_2O_5 and their Application to Optical Waveguides, by Bei Zhang, Siamak Forouhar, S . Y. Huang and William S. C. Chang (supported by AFOSR Grant No. 80-0037, NSF Grant No. ECG-8102927 and AFOSR Grant No. 80-0056, submitted to IEEE Journal of Lightwave Technology). Properties of C_2F_6 (freon 116) reactive ion beam etching (RIBE) of both $LiNbO_3$, Ti-indiffused $LiNbO_3$ and sputter deposited Nb_2O_5 film in $LiNbO_3$ waveguides are reported here. A differential etching rate of approximately 4:1 has been measured for etching Ti-indiffused $LiNbO_3$ and AZ1350B Shipley photoresist, respectively. We have used this etching technique to fabricate diffraction gratings on both Ti-indiffused $LiNbO_3$ and Nb_2O_5-$LiNbO_3$ waveguides with measured efficiencies in excess of 85%.

7. Ion Beam Etching of BaO Glass and SiO_2 Thin Films and Their Application to Optical Waveguides (supported by AFOSR Grant No. 80-0037 and NSF Grant No. ECG-8102927, accepted for publication in Applied Optics). In this work we

report the results on the etching of SiO_2 and BaO glass film by Ar ion milling and C_2F_6 RIBE. Differential etching rates of approximately 4:1 for etching BaO glass and AZ1350B photoresist have been measured. Submicron resolution, maximum groove depth of 6,000 A and high efficiency (75%) have been obtained in the application of this etching technique to fabricate grating lenses on BaO glass waveguides.

8. Design and Fabrication of Efficient Diffraction Transmission Gratings on Step Index Optical Waveguides, by Jean-Marc Delavaux and William S. C. Chang (supported by AFOSR Grant No. 80-0037, to be submitted for publication). Here we report the fabrication and the evaluation of high efficiency and low loss constant periodicity gratings on single mode planar waveguides. For the design of both etched and deposited gratings, the coupling coefficient has been found to be given by $k_c = \Delta n_{eff}/(\lambda_o/2)$. Investigation of the Δn_{eff} value has shown that, for small groove height, larger Δn_{eff} can be obtained for CeO_2 deposited grooves than for etched grooves. In grating structures where Q and ρ factors are high, there is good agreement between the experimentally measured characteristic and the prediction from the conventional coupled mode theory. However, a more rigorous coupled mode analysis is necessary for low ρ factor cases. Minor variations in the fabrication processes (e.g. $\Delta n = 0.02$) may cause the diffraction efficiency to vary as much as 15%, while the angular field of view does not ssem to be affected by process variations.

9. Experimental Evaluation of the Efficiencies of Transmission Diffraction Gratings on Planar Optical Waveguides, by Jean-Marc Delavaux, William S. C. Chang (UCSD) and M. G. Moharam (Georgia Institute of Technology)

(work at UCSD supported by AFOSR Grant No. 80-0037, manuscript in preparation). In this paper we compared the theoretical results of conventional coupled mode theory with that of the rigorous coupled mode theory by experimentally fabricating and evaluating the constant periodicity transmission gratings on BaO glass waveguides. We have found that (a) The rigorous coupled mode theory gives an accurate prediction of the diffraction efficiency both in the Bragg regime ($Q > 10$) and in the transition regime ($1 < Q < 10$). According to this theory high diffraction efficiency can be obtained at low Q, thereby opening up the potential for obtaining simultaneously large angular field of view with high efficiency. (b) The conventional coupled mode theory is accurate only in the Bragg regime. (c) For gratings with high diffraction efficiency, either the Q or the ρ factor can be used as the criterion for predicting the absence of higher orders of diffraction. (d) For gratings with low efficiency, the ρ factor should be used to estimate the upper bound of the power diffracted into the higher orders.

10. Fundamental Limitations in the Performance of Chirped Grating Lenses on Planar Optical Waveguides, by Jean-Marc Delavaux and William S. C. Chang (work supported by AFOSR Grant No. 80-0037, manuscript in preparation). Limitations in the diffraction efficiency of linearly chirped grating lenses on planar waveguides as the F number is lowered have been calculated by the generalized coupled mode theory. This decrease in efficiency is caused by phase distortions at the output of the linearly chirped grating lens. For a given F number, the loss of diffraction efficiency can be reduced by using a larger coupling coefficient in a linearly chirped grating lens or by using a parabolic curved chirped grating lens to reduce the phase distortions.

Limitations in the performance of chirped grating lenses caused by fabrication tolerances have also been discussed. Experimental confirmation of the theoretical predictions have been obtained.

The preceeding papers are alaso used for the Ph.D. dissertations of Siamak Forouhar and Jean-Marc Delavaux. The completed dissertation of Siamak Forouhar is included here as a technical report. The second dissertation by Jean-Marc Delavaux will be forwarded to AFOSR as soon as it is completed. Since all the papers will be published these two reports will not be generally distributed.

3. Research on Electro-Refraction Effect in III-V Compound Semiconductors

The goal of our work so far has been to quantitatively evaluate the electro-optical properties (i.e. the refractive index n and the absorption coefficient α) of III-V compound semiconductors as a function of the applied electric field at various wavelengths λ near the wavelength λ_g corresponding to the bandgap. We must measure experimentally the variation of the refractive index n with the electric field (i.e. electro-refraction) and the variation of the absorption coefficient α with the electric field (i.e. electro-absorption) of different binary, ternary and quaternary alloy semiconductors such as GaAs, InP, InGaAs, etc. in order to design electrooptical modulators, multipliers, logic gates, etc. as discussed in the proposal.

In order to evaluate n and α as a function of wavelength λ, a tunable laser source is required. For wavelengths in the visible spectrum our source is a tunable dye laser. For infrared wavelength our source is an optical parametric oscillator pumped by the dye laser. In order to determine a small change of refractive index, we have chosen to measure the refractive index n

interferometrically. We have considered three types of interferometers, Fabry-Perot, Michelson and Mach Zehnder and constructed both the Fabry-Perot and the Mach-Zehnder interferometers.

Since a high finesse Fabry-Perot interferometer has very sharp transmission peaks it is expected to be a very sensitive device. However, the finesse drops as the absorption inside the interferometer increases when λ gets closer to λ_g and the high sensitivity is lost. In addition, the coherence length of a dye laser is fairly short, thus, the reflectors of the Fabry-Perot interferometer must be very close to each other in order to get high visibility for the fringes. There is very little room to mount the semicondutor sample between the reflectors.

A Michelson interforometer has two independent arms, so that absorption due to the sample in one arm can be balanced by a variable attenuator in the other arm. As long as the difference of the optical paths in the two arms is small, the visibility of the interference fringes will remain high, even for radiation with short coherence length. One disadvantage of the Michelson interferometer is that the light must travel the same path twice. This means that the sample will absorb the light twice. The Mach-Zehnder interferometer also has two independent arms like the Michelson, but the beam travels only once through each arm. We have used the Mach-Zehnder interferometer illustrated schematically in Figure 2 for our measurements made so far.

The experimental method is as follows. An optically polished semiconductor sample is placed in one arm of the interferometer. In the other arm there is an attenuator (to be used if necessary). As the refractive index of the specimen is changed either as a consequence of the change in wavelength of the source or as a result of an applied electric field to the specimen the fringe position shifts. By counting the number of times the fringes take a

complete "step", we measure the phase change and thus the change in the refractive index. Notice that in the interferometric method, only changes in the refractive index can be measured, the index cannot be determined absolutely. In order to apply the electric field initially, indium tin oxide transparent electrodes are r.f. sputtered on both sides of an optically polished semiconductor sample. It is to be expected that the indium-tin oxide produces a barrier estimated to be about 0.8 eV on large bandgap semiconductors such as GaAs. It is desirable to establish the nonlinear refractive properties of such materials as a function of their ir rfacial properties as well as a function of the bulk properties. For th reason ohmic contacts (such as 20% Ge in 80% Au eutectic) may be applie ' vacuum deposition and alloying procedures to form thin transparent layers (less than 100 A in thickness). In order to reduce the heat dissipation in the sample, a pulsed voltage is applied to the electrode, triggered in synchronization with the laser radiation pulse. The voltage pulse duration is much longer than the laser pulse duration so that the voltage is relatively constant with respect to jitters in the laser pulse.

So far the refractive indicies of two materials have been measured. Figure 3 shows the measured dispersion $dn/d\lambda$ as a function of wavelength for the indirect III-V compound semiconductor GaP near the bandgap. The dispersion predicted by the single effective oscillator theory is shown as the solid curve. Note that the data fit the theoretical curve quite well when λ is far away from λ_g. Near the bandgap there is an additional amount of dispers on related to the sudden increase in absorption. Since GaP has an indirect bandgap, the rapid change of Δn is absent. Figure 4 shows the change in the refractive index of semi-insulating GaAs as a function of the applied electric field for several wavelengths near its bandgap. Each curve stops

where absorption is so high that interference fringes disappear. Note that for λ = .885 μm, the change in index is 0.006 for an applied electric field of 7 kV/cm. To match this performance, a linear electrooptical modulator operating in the longitudinal mode would have to have a half wave voltage $V\pi \approx 50$ V. By comparison, the best ferroelectric single crystalline material, $LiNbO_3$ has a $V\pi \approx 1300$ V.

However, it was subsequently seen that the very large electro-refraction effect as observed by us in Figure 4 happened after what appeared to be an electrical breakdown in the GaAs material. We have found that the electro-refraction effect observed before the apparent electrical breakdown is about 10 times smaller but is still larger than that of lithium niobate. We operated some samples below the "breakdown" voltage and the changes in index of these samples are compared in Figure 5. In No. 1 and No. 3 samples we had InSnO electrodes and in No. 2 sample we had Au-Ge electrodes so that we could compare the effect of these types of electrode. In the first No. 1 sample the electro-refractive effect appeared to be fairly large (0.001 index change for an applied electric field of 10 Kv/cm). Even though sample Nos. 2 and 3 consisted of two different types of electrodes, electro-optically they appeared to behave similarly. However, the electro-refraction effect in the later two cases was comparatively small and the precision of the determination of the fringe shift was limited by the sensitivity of the "fringe-counting" measurement scheme.

In order to design devices, components, and systems associated with both electro-refraction and electro-absorption, we need to understand and to make precise quantitative estimations of both these effects. At this stage of our experiments we are not exactly clear as to how to interpret our data. It is suspected that the thermal effects, carrier injection and trapping of

electrons in localized states in the semiconductor could all play a role in the process of electrical field induced index change. These effects are also expected to be associated with the apparent "breakdown" process and the behavior of the material after the "breakdown". Understanding the properties of these effects are obviously important as they could slow down the switching speed of the devices of interest. Thus, we have decided to find new methods to measure the electro-refraction effect with much less applied electric voltage and with a different material such as InGaAs. One method is to improve the sensitivity of our measurement system so that we can measure a small amount of phase shift created at a low applied voltage. The second method is to measure the phase shift over a long path length, e.g. in an optical waveguide, so that a small change in index can produce a large phase shift.

We have now modified our interferometer monitoring system to give improved sensitivity. We use a silicon photo detector bicell to monitor the sinusoidal intensity variation of the interferometer output. The bicell consists of two rectangular photo detectors on a single chip separated by a small gap. If the bicell surface is exposed to the intensity variation of the interference fringe the difference I_B-I_A in the electrical output currents of the two cells will be proportional to the sine of the spatial phase variatoin of the interference fringe pattern. This difference in current will be amplified and sampled by a 12 bit analog to digital converter which is interfaced with a computer. Thus, the bicell will be able to detect a small shift of the interference fringe pattern. We expect this measuring system to be at least 10 times more sensitive than the fringe counting method. The

system will further enable us to isolate slow switching processes and to determine whether the electro-refraction effect observed is truly electronic in nature.

Work is in progress to fabricate optical waveguides and to measure the electro-optical refraction effect in optical waveguides, especially in GaInAs/InP.

4. PAPERS PRESENTED, PUBLISHED AND SUBMITTED

W. S. C. Chang and P. R. Ashley, "Fresnel Lenses in Optical Waveguides", IEEE J. Quantum Electron., QE-16, 744 (1980).

Z-Q. Lin, S. T. Zhou, W. S. C. Chang. S. Forouhar and J. Delavaux, "A Generalized Two-Dimensional Coupled-Mode Analysis of Curved and Chirped Periodic Structures in Open Dielectric Waveguides", MTT Transactions, MTT-29, 881 (1981).

W. S. C. Chang, Z-Q. Lin, S. T. Zhou, J. Delavaux and S. Forouhar, "The Feresnel and Chirped Grating Lenses in Optical Waveguides", Proceedings of SPIE Technical Symposium, Vol. 269, p.105, North Hollywood, 1981 (February).

S. Forouhar and W. S. C. Chang, "Analysis of Chirped Grating Lenses", 1980 IEEE MTT-S International Microwave Symposium, May 28th-30th, 1980, Washington, D.C.

W. S. C. Chang, Z-Q. Lin, S. T. Zhou, J. Delavaux and S. Forouhar, "The Fresnel and Chirped Grating Lenses in Optical Waveguides", SPIE Technical Symposium, Los Angeles, 1981 (February).

Z-Q. Lin, S. T. Zhou, W. S. C. Chang, S. Forouhar and J. Delavaux, "A Generalized Two-Dimensional Coupled-Mode Analysis of Curved and Chirped Periodic Structures in Open Dielectric Waveguides", MTT International Symposium, Los Angeles, 1981 (June).

W. S. C. Chang, S. T. Zhou, Z-Q. Lin, S. Forouhar and J. M. Delavaux, "Performance of Diffraction Lenses in Planar Optical Waveguides", The Third International Conference on Integrated Optics and Fiber Optics, Communications, San Francisco, 1981 (April).

W. S. C. Chang, "The Effects of Materials Technology and Fabrication Tolerances on Guided-Wave Optical Communication and Signal Processing", a Chapter of the book: VLSI Electronics Microstructure Science, Vol.3, Norman Einspruch (Editor), Academic Press (1981).

J. Delavaux, S. Forouhar, W. S. C. Chang and R. X. Lu, "Experimental Fabrication and Evaluation of Diffraction Lenses in Planar Optical Waveguides", paper submitted to IEEE/OSA CLEO '82, April 14th-16th, 1982, Phoenix, Arizona.

W. S. C. Chang, S. Forouhar, J. Delavaux, R. X. Lu, "Fabrication and Performance of Diffraction Lenses", SPIE Technical Symposium, Los Angeles, California, January 28th-29th, 1982.

J-M. Delavaux, S. Forouhar, W. S. C. Chang and R. X. Lu, "Experimental Fabrication and Evaluation of Diffraction Lenses in Planar Optical Waveguides", paper submitted to IEEE/OSA CLEO '82, April 14th-16th, 1982, Phoenix, Arizona.

W. S. C. Chang, S. Forouhar, J-M. Delavaux, R. X. Lu, "Fabrication and Performance of Diffraction Lenses", SPIE Technical Symposium, Los Angeles, California, January 28th-29th, 1982.

J-M. Delavaux, S. Forouhar, W. S. C. Chang and R. X. Lu, "Experimental Fabrication and Evaluation od Diffraction Lenses in Planar Optical Waveguides", paper submitted to IEEE/OSA CLEO '82, April 14-16th, 1982, Phoenix Arizona.

W. S. C. Chang, S. Forouhar, J-M. Delavaux, R. X. Lu, "Fabrication and Performance ofd Diffraction Lenses", SPIE Technical Symposium, Los Angeles, CA, January 28-29th, 1982.

W. S. C. Chang, S. Forouhar, J-M. Delavaux, C. Warren and R.-X. Lu, "Chirped Grating Lenses in Ti-Indiffused $LiNbO_3$ Optical Waveguides". Paper presented at the European Conference on Optical Systems and Applications, 7th-10th, September, 1982, Edinburgh, Scotland. Published in the Proceedings of the ECOSA'82, SPIE Vol.369, pp.581-590, 1982.

C. Warren, S. Forouhar and W. S. C. Chang, "Double Ion-Exchanged Chirped Grating Lens in Lithi$_u$m Niobate Waveguides" Appl. Phys. Lett., 43, 424-426, 1982.

S. Forouhar, R.-X. Lu, W. S. C. Chang, R. L. Davis and S. K. Yao, "Chirped Grating Lenses on Nb_2O_5 Transition Waveguides", Appl. Optics, 22, 3128-3132 (1983).

S. Forouhar, W. S. C. Chang and S. K. Yao, "Chirped Grating Lenses in Ti-Indiffused $LiNbO_3$ Planar Waveguides", 4th International I.A.O.C. Conference, Tokyo, Japan, June 27-30th, 1983.

T. Findakly and S. K. Yao, "Chirped Grating Lenses on $LiNbO_3$ by Benzoic Acid Treatment", 4th International I.O.O.C. Conference, Tokyo, Japan, June 27-30th, 1983.

5. Persons Supported in this Grant During FY'82

1. William S. C. Chang, Professor
2. Siamak Forouhar, Graduate Assistant
3. Jean-Marc Delavaux, Graduate Assistant
4. Timothy Van Eck, Graduate Assistant
5. L. M. Walpita, Assistant Research Physicist
6. Christopher Warren, Graduate Assistant
7. Interactions and coupling with other groups.

The researchers are most appreciative of the collaboration with the NSF supported National Research Facilities on Submicron Structures at Cornell University (NSF Grant ECS-8200312). All the masks are made by the EBMF-11 Electron Beam pattern generator at Cornell.

Ron Xin Lu is a visiting scholar from Chengtu Institute of Radio Engineering, People's Republic of China. He is not supported by this grant. However, he has carried out the work of the reactive sputtering of Nb_2O_5 film and the sputtering of glass waveguides.

Beginning FY83, a research contract was awarded jointly to TRW Technology and Research Center, El Segundo, California and UCSD by the Air Force Avionics Laboratory, WPAFB, for developing a chirped grating lens on $LiNbO_3$ for r.f. spectrum analysis, Contract No. F33615-82-6-1751. This represents a successful transfer of the 6.1 basic research results into a 6.2 applied research program to be jointly conducted by industry and the University.

BRAGG DIFFRACTION

CHIRPED GRATING LENS

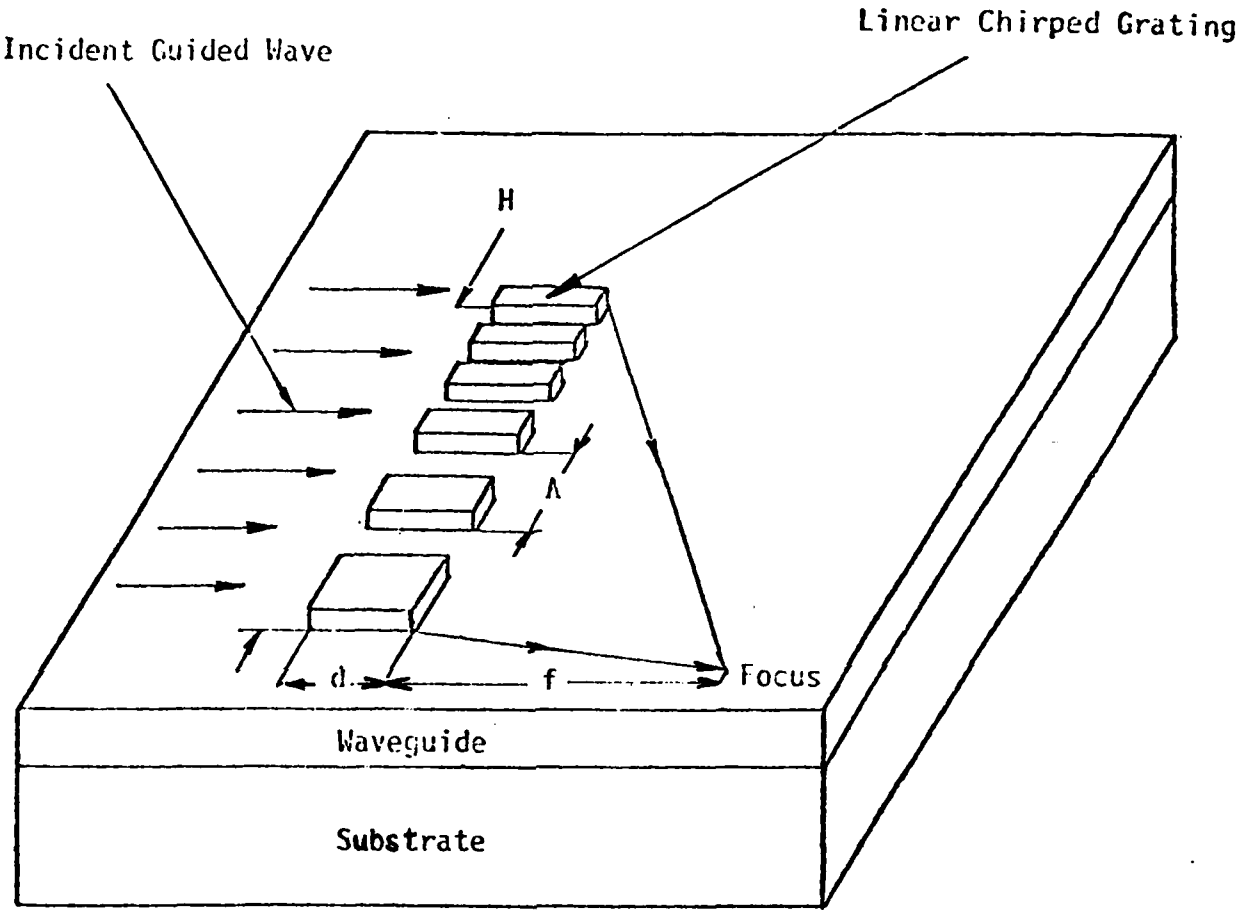

TYPICAL DIMENSIONS OF A GRATING LENS

d = (15 - 400 μm)

Λ = (1 - 20 μm)

H = (1 to several mm)

f = (5 - 30 mm)

Figure 1

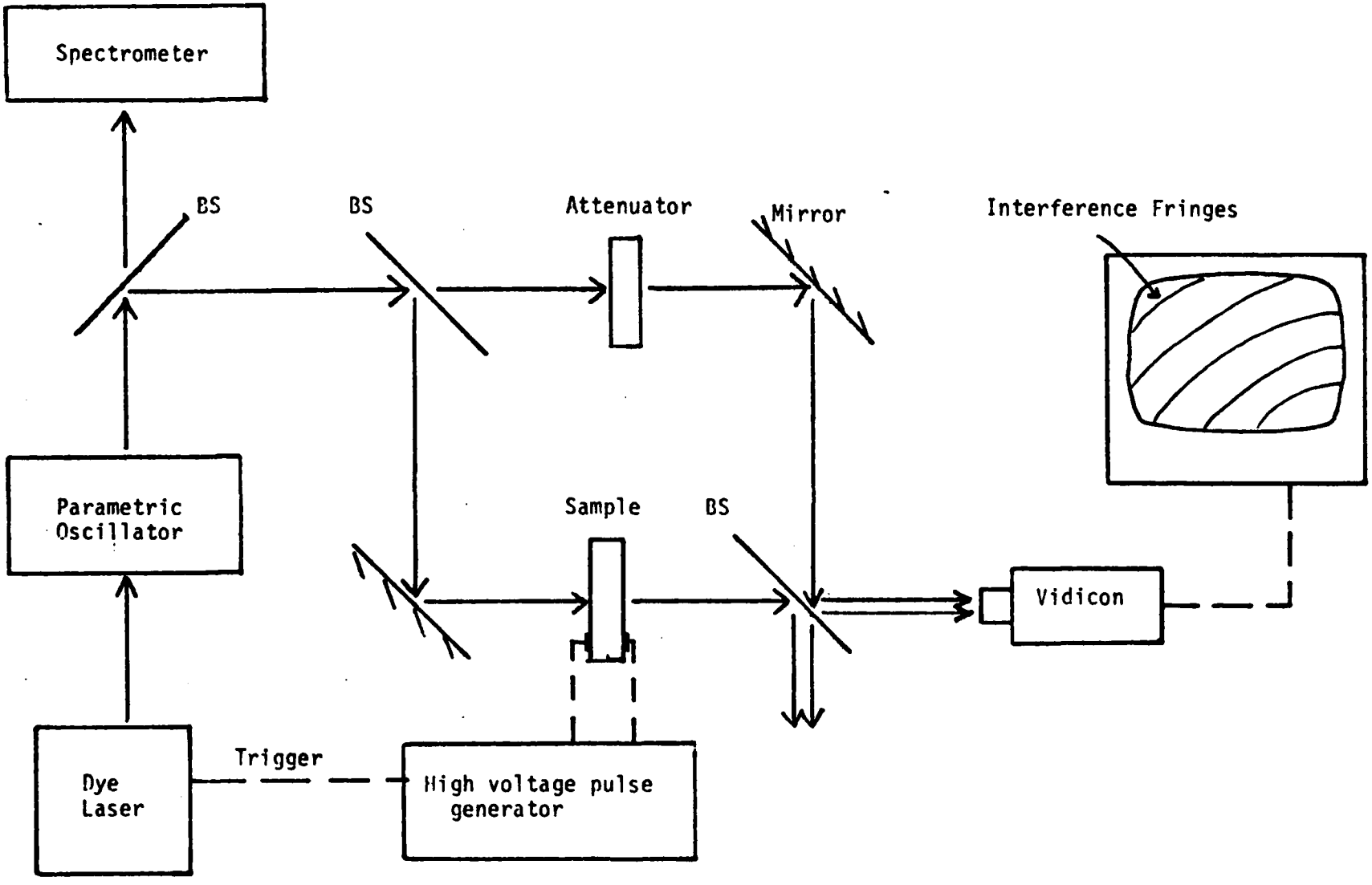

Figure 2 Experimental setup with Mach-Zehnder Interferometer

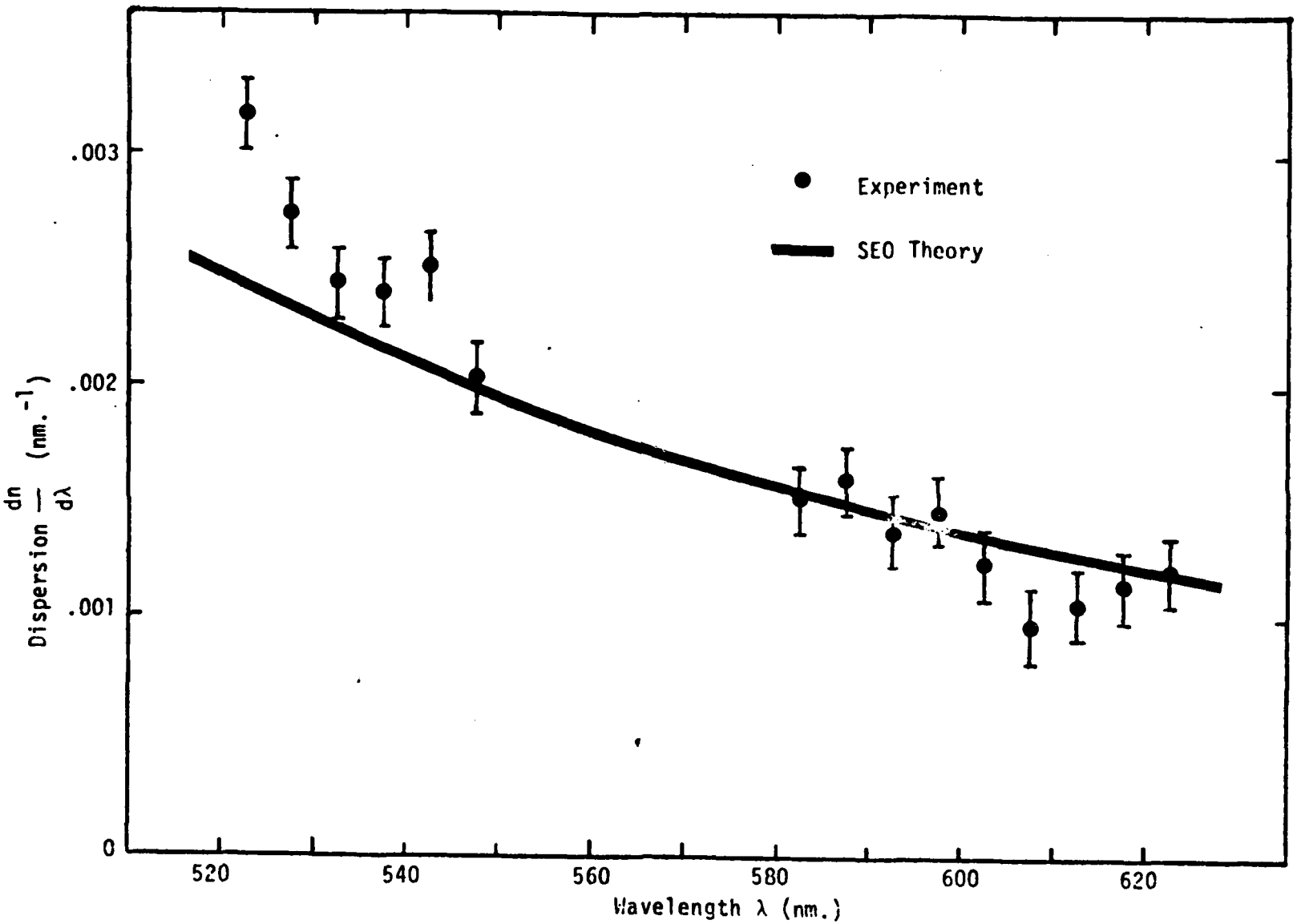

Figure 3 Dispersion of Gallium Phosphide.

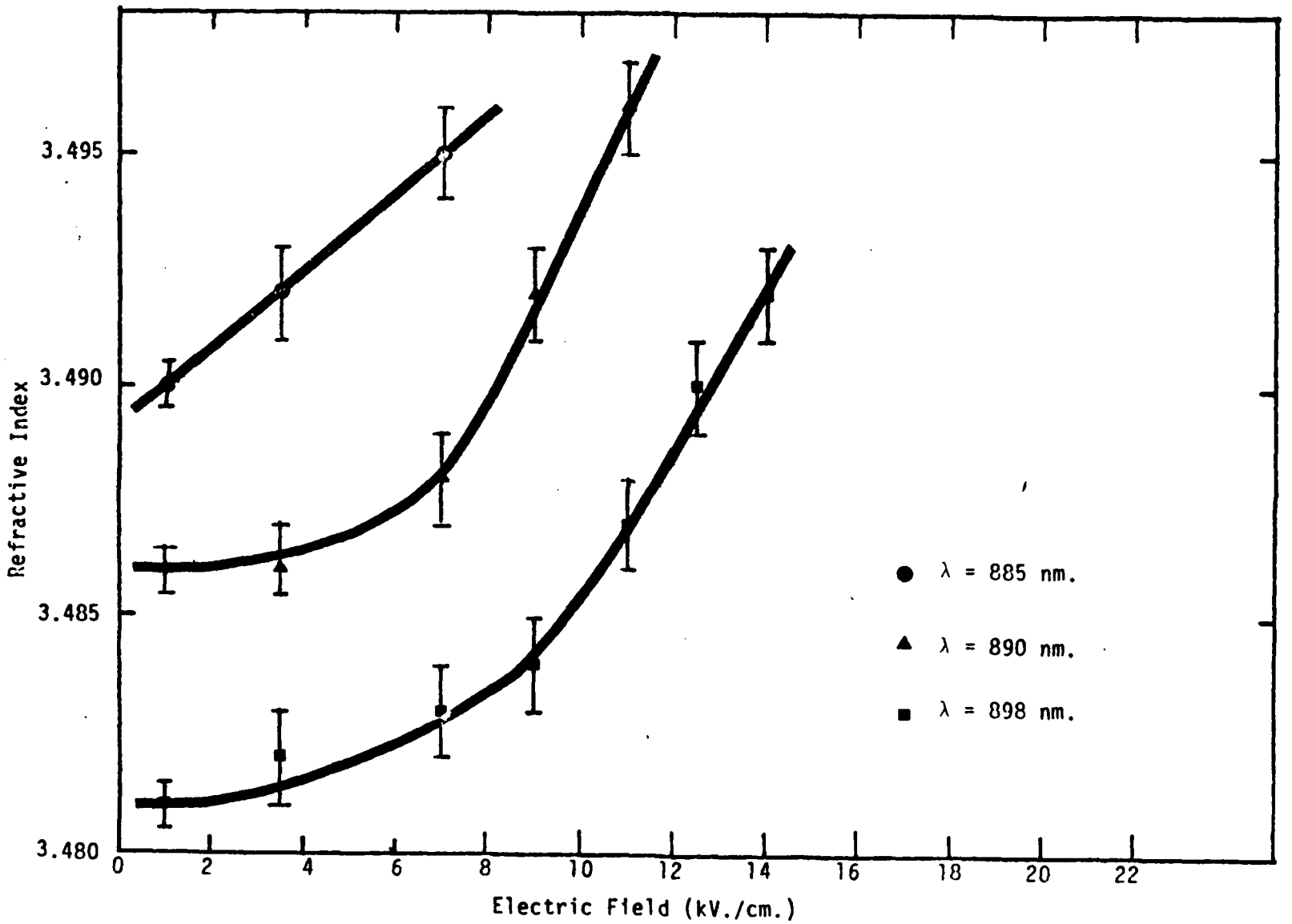

Figure 4 Change of Refractive Index of Semi-insulating Gallium Arsenide due to Electric Field

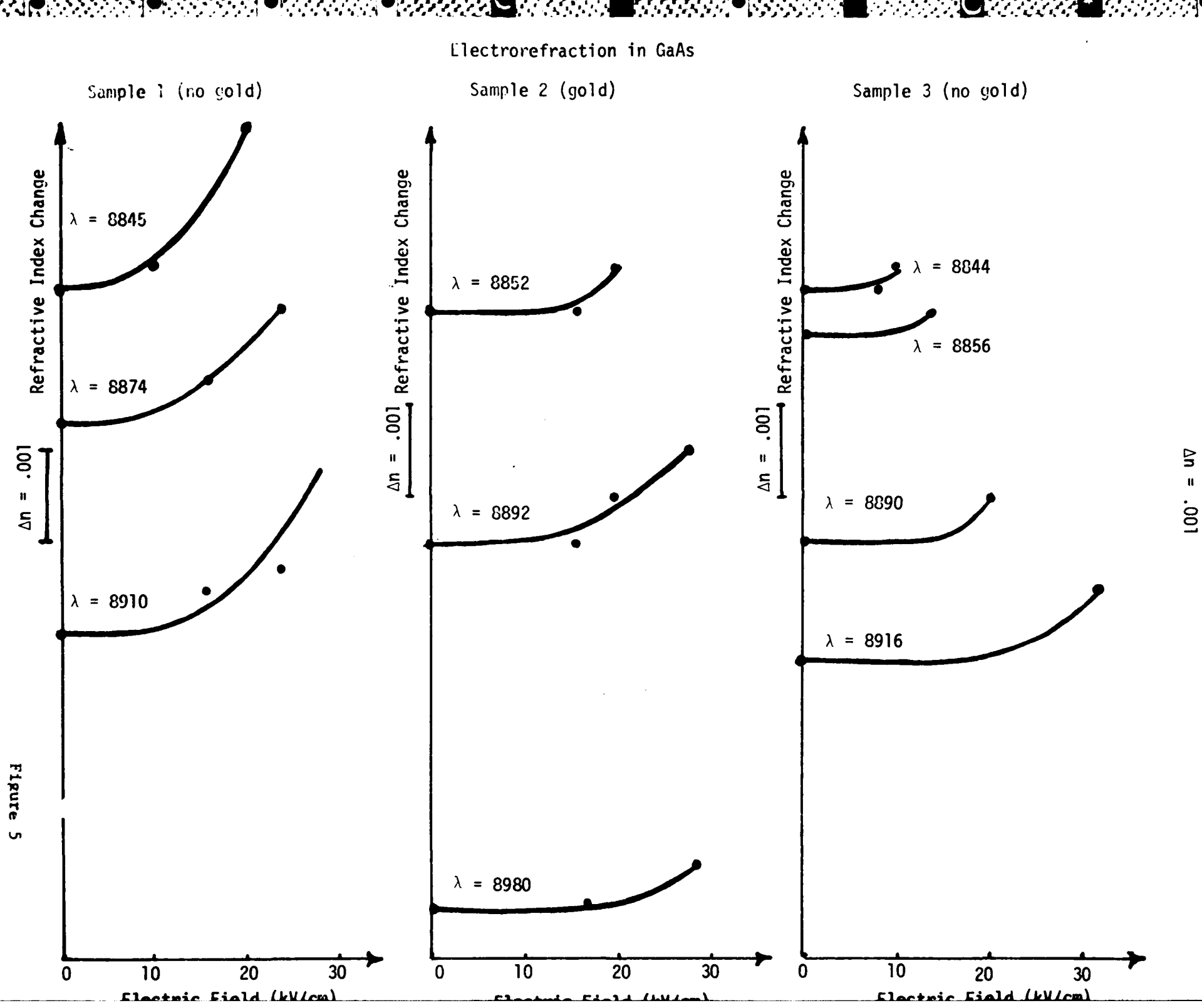
Electrorefraction in GaAs
Sample 1 (no gold)
Sample 2 (gold)
Sample 3 (no gold)
Refractive Index Change
Δn = .001
λ = 8845
λ = 8874
λ = 8910
λ = 8852
λ = 8892
λ = 8980
λ = 8844
λ = 8856
λ = 8890
λ = 8916
0
10
20
30
Electric Field (kV/cm)

Figure 5

Double ion exchanged chirp grating lens in lithium niobate waveguides

Christopher Warren, Siamak Forouhar, and William S. C. Chang
C-014, Department of Electrical Engineering and Computer Sciences, University of California, San Diego, La Jolla, California 92093

S. K. Yao
TRW Technology Research Center, El Segundo, California 90245

(Received 19 April 1983; accepted for publication 13 June 1983)

An integrated optical chirped grating lens has been produced which exhibits high throughput efficiency (75%) and large angular field of view (3°). The waveguide substrate is x-cut lithium niobate, and ion exchange in benzoic acid is the method used for making the lens and the waveguide.

PACS numbers: 42.82. + n, 42.80.Lt, 42.80.Fn, 42.78.Cf

Chirped grating lenses on glass optical waveguides have been fabricated successfully with 90% diffraction efficiency, several degrees angular field of view, and near diffraction limited performance.[1,2] However, for some signal processing applications, such as the rf spectrum analyzer, it is necessary to fabricate these lenses on $LiNbO_3$ waveguides. The fabrication and performance of chirped grating lenses on commonly used $LiNbO_3$ waveguides, i.e., Ti-indiffused $LiNbO_3$, has recently been reported,[3] and a throughput efficiency of 60% with 2° angular field of view was obtained. However, the combination of high efficiency and large angular field of view for chirped grating lenses on Ti-indiffused $LiNbO_3$ waveguides is difficult to obtain due to two reasons:

(a) The mode index of Ti-indiffused $LiNbO_3$, n_e, is close to the substrate index n_s, so the substrate mode coupling may limit the maximum angular field of view or the efficiency of small F-number grating lenses.

(b) The Ti-indiffused $LiNbO_3$ waveguides have large mode depth.[3] The large mode depth implies small coupling coefficient, thus a large diffraction efficiency grating requires long grating grooves which limit the angular field of view.

Furthermore, since lithium niobate has a high index, the overlay film material used for grating must have an even higher index in order to obtain large coupling coefficient at small film thicknesses.

In order to improve the chirped grating lens performance and relax the limitation imposed by the Ti-indiffused $LiNbO_3$ waveguides, we have investigated the single mode waveguide in $LiNbO_3$ made by proton ion exchange.[4] Compared to the Ti-indiffused waveguide, it has smaller mode depth and larger mode index. We have obtained higher performance chirped grating lenses on an ion-exchanged waveguide by a second ion exchange process.

A typical chirped grating lens is illustrated in Fig. 1. There are several factors which one should consider when choosing a particular chirped grating lens design. From the generalized coupled mode theory,[5] in order to have a large diffraction efficiency we can choose $Kd \sim \pi/2$, where K is the coupling coefficient and d is the grating groove length. The coupling coefficient is directly related to the change in effective index, Δn_e, in the waveguide caused by the grating grooves. In the case of small effective index perturbations this relationship is given by[5] $K = \pi \Delta n_e / \lambda$.

Another requirement that must be satisfied for large diffraction efficiency is that the gratings must not scatter heavily into either the higher diffraction orders or the substrate modes. A common figure of merit in this regard for constant periodicity grating is the dimensionless parameter Q,[6] $Q = 2\pi\lambda d/(n_e \Lambda^2)$, where λ is free-space wavelength and Λ is periodicity of grating. For a chirped grating where Λ is variable, we shall have a local Q factor for various sections of the lens. For most of our designs, we have kept the local Q value larger than 5 so that the energy diffracted into higher orders may be ignored. Optical loss due to conversion into the substrate modes can be minimized if n_e can be made significantly larger than n_s.

A third consideration in lens design is the angular field of view, $\Delta\theta$. From the conventional coupled mode theory, the $\Delta\theta$ of a constant periodicity grating is given by $\Delta\theta \approx \Lambda / d$.[6] This relationship can still serve as a useful qualitative

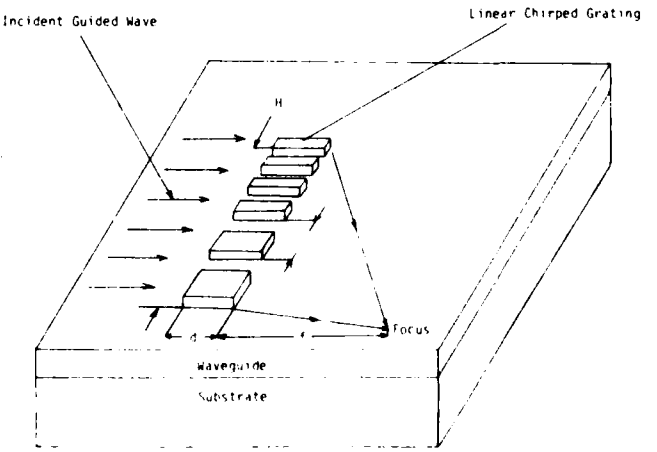

FIG. 1. Chirped grating lens structure and the typical ranges of the design parameters used

 0003-6951/83/170424-03$01.00

guide for the design of a chirped grating lens. For large $\Delta\theta$, we want Λ/d large. But for large Q, we want d/Λ^2 large. Thus, we should use as small a Λ as the resolution of the lithographic process allows, while using a large enough K such that the optimum d for high efficiency is still small enough to support large $\Delta\theta$, yet is not so small for Q to become too low.

As was mentioned previously, substrate mode coupling in Ti-indiffused waveguides may limit $\Delta\theta$ or the efficiency of small F-number grating lenses. This is because for small F number a significant portion of the input beam will not be at Bragg angle due to the chirped periodicity of the grating. In other words, only within a small range of Λ along the lens (usually at the middle) will Bragg's diffraction condition be satisfied approximately. For significant deviations from Bragg angle, there will be substrate mode conversion if the mode index n_e of the waveguide is not significantly larger than the substrate index n_s.

The proton ion-exchange process is expected to give an n_e significantly higher than n_s. The second proton ion exchange is expected to give a large K for the grating grooves. Thus, high performance chirp grating lens can be expected with a double proton ion-exchange process.

The ion-exchange method used here involves dipping a sample of X-cut $LiNbO_3$ in molten benzoic acid[4] held in a furnace that has a $\pm 1°$ temperature control. Some of the protons from the acid diffuse into the lithium niobate and replace some of the lithium ions in the crystal. The result is that a thin surface layer of the crystal acquires a constant refractive index of 2.32, which is large compared to the substrate index, 2.20 (at $\lambda = 0.6328\,\mu$m). This index profile and index value can be determined by fitting the index profile with measured effective indicies of a multimode waveguide by WKB approximation. The temperature and duration of immersion control the depth of this layer, the mode indices, and the number of modes. We work strictly in the single mode region. In Fig. 2, a theoretical curve of TE_0 mode index versus time of immersion at 217 °C, is given, based upon Jackel's reported diffusion coefficient of $0.37\,\mu m^2/h$, as well as two other values of diffusion coefficients for comparison. The discrete points are the experimentally observed waveguide index n_e. They are approximately in agreement.

An aluminum mask in the form of chirped grating grooves is made on the single-mode ion-exchanged waveguide by the lift-off method, contact printed from a flexible chromium mask. The aluminum serves as a protective mask during the second ion exchange. For the second ion exchange, the waveguide is immersed in benzoic acid for a few minutes at 204 °C. Thus, the majority of the planar waveguide is double ion exchanged, while the regions beneath the aluminum fingers is single ion exchanged. After the second ion exchange the aluminum mask is removed by chemical etching.

Double ion-exchange produces a change in n_e from the single ion exchange. In order to measure Δn_e, we have set aside a portion of the waveguide which is also covered by aluminum during the second ion exchange. Δn_e is measured by the change in coupling angles of the light beam into the rutile prism in the single exchanged region and in the double exchanged region. A theoretical curve of Δn_e versus second ion exchange time is plotted in Fig. 3 using $D = 0.12\,\mu m^2/h$. The experimental points are marked by the squared dots. Clearly there are some variations of Δn_e caused by some unknown variations of our experimental conditions. Nevertheless, the averaged Δn_e may be described by $\Delta n_e = 0.0012t$, where t is the second ion-exchange time in minutes at 204 °C.

All optical measurements are performed with a He-Ne laser through rutile prism couplers. The throughput efficiency is defined as the ratio of the optical power in the focused diffracted guided wave beam to the power in the transmitted guided optical beam when the incident beam is

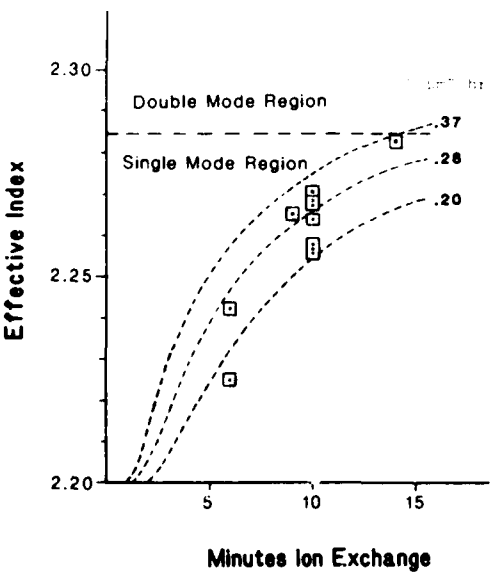

FIG. 2. Effective index of ion-exchanged $LiNbO_3$ waveguides vs time of immersion in benzoic acid, $T = 217$ °C. The dashed lines show the use of different coefficients used in theoretically modelling the waveguides.

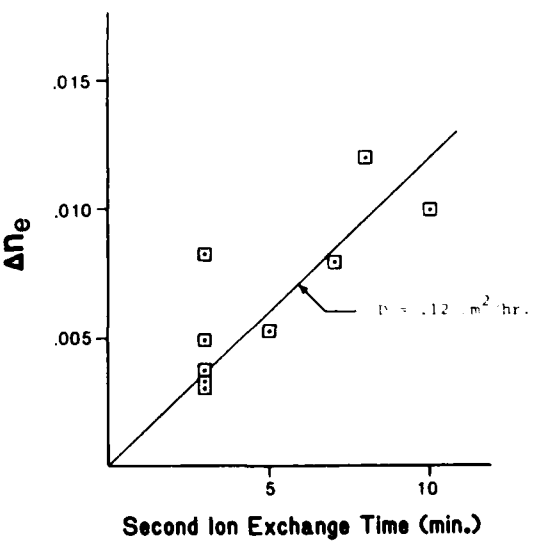

FIG. 3. Waveguides of Fig. 2 with $n_e = 2.265 \pm 0.05$ were ion exchanged a second time. The change in effective index is plotted vs time of second ion exchange at $T = 204$ °C.

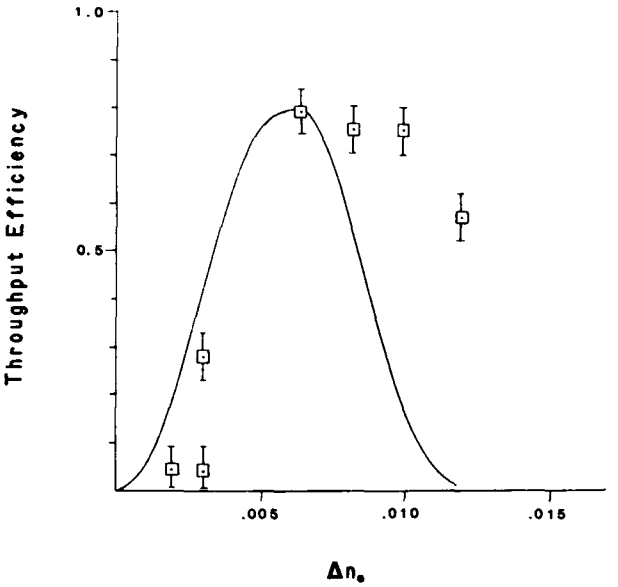

FIG. 4. Throughput efficiency vs Δn_e for the chirped grating lens made in $LiNbO_3$ waveguides.

moved transversely to bypass the lens. The diffraction efficiency is the ratio of the power measured in the focused beam to the sum of the powers measured in all the orders of diffraction. So far, within the accuracy of our measurement the diffraction efficiency is always equal to the throughput efficiency, implying very little power converted by the lens into the substrate modes. However, the average attenuation rate of the single mode ion-exchanged waveguide is 3 dB/cm. There are significant amounts of light power appearing in the substrate and in the tails of the output m line, indicating that the random scattering noise of the ion exchanged waveguide will be higher than that of the Ti-indiffused waveguide.

Figure 4 shows the measured throughput efficiency η for various Δn_e created on seven different samples. In all these samples, the n_e of the TE_0 mode produced in the first ion exchange is 2.265 ± 0.005. The lens has the same mask pattern, $\Lambda_{min} = 1.73\ \mu m$, $\Lambda_{max} = 3.45\ \mu m$, focal length $(f) = 12$ mm, grating groove length $d = 80\ \mu m$, lens width $(h) = 1$mm, and $F = 12$. The solid curve represents the efficiency variation calculated from the generalized coupled mode theory for $K = \pi \Delta n_e / \lambda$. Clearly, the measured efficiency at Δn_e larger than 0.007 is larger than the calculated efficiency, implying an experimental K value smaller than that given by $K = \pi \Delta n_e / \lambda$. A reduction in K value could occur due to mechanisms such as lateral diffusion in the z-axis direction. The exact mechanism for the shift of the experimental points is still being investigated. However, the experimental results have demonstrated that the second ion-exchange process is more than sufficient to generate the large Δn_e required for obtaining high efficiency at short d values.

By measuring the diffraction efficiency as a function of the angle of incidence of the input guided wave beam, we obtain experimentally the angular field of view $\Delta\theta$ to be in the range from 2.4° to 3.2°. $\Delta\theta$ is defined as the change in incidence angle within which the measured efficiency is larger than one-half the highest efficiency. We do not know yet the exact reason for the variation in $\Delta\theta$. It may be caused by the tolerance of the fabrication processes.

In conclusion, we have demonstrated a chirped grating lens on $LiNbO_3$ that has high efficiency (75%) and large angular field of view (3°). It is potentially feasible to obtain a higher efficiency and a larger angular field of view than the data reported here by searching for a smaller d without higher orders of diffraction and by controlling the second ion exchange more precisely to obtain the desired K. There seem to be two drawbacks to ion-exchanged waveguides: (1) they have a larger scattering loss than that of the Ti-indiffused waveguides; (2) n_e and Δn_e will change if the sample is heated to 200 °C.

This work is supported in part by AFOSR grant No. 80-0037. The grating lens mask is made by electron beam lithography at the submicron facility of Cornell University under NSF grant No. ECS-8200312.

[1]J. M. Delavaux, Siamak Forouhar, W. S. C. Chang, and R. X. Lu, "Experimental Fabrication and Evaluation of Diffraction Lenses in Planar Optical Waveguides," IEEE/OSA Conference on Lasers and Electro-Optics, April 1982, Phoenix, Arizona.
[2]S. K. Yao and D. E. Thompson, Appl. Phys. Lett. **33**, 635 (1978).
[3]W. S. C. Chang, Siamak Forouhar, Jean-Marc Delavaux, Christopher Warren, and Ron-Xin Lu, "Chirped Grating Lenses in Ti-indiffused $LiNbO_3$ Optical Waveguides," paper presented at ECOSA '82 Conference, Edinburgh, Scotland, September 1982.
[4]J. L. Jackel, C. E. Rice, and J. J. Vaselka, Jr., "Proton Exchange for High Index Waveguides in $LiNbO_3$," IEEE/OSA Topical Meeting in Integrated and Guided Wave Optics, January 1982, Pacific Grove, CA.
[5]Richard P. Kenan, J. Appl. Phys. **46**, 4545 (1975).
[6]Herwig Kogelnik, Bell Syst. Tech. J. **48**, 2909 (1969).

Reprinted from **Applied Optics**, Vol. 22, page 3128, October 1, 1983

Chirped grating lenses on Nb_2O_5 transition waveguides

Siamak Forouhar, Ron-Xin Lu, William S. C. Chang, Richard L. Davis, and Shih-Kay Yao

Efficient tapered Nb_2O_5 transition waveguide obtained by reactive sputtering has been demonstrated experimentally. It provides effective interconnection between two sections of Ti-indiffused waveguide with 0.8-dB total insertion loss. Chirped grating lenses have also been fabricated on Nb_2O_5 waveguides that have yielded 85% throughput efficiency. For signal processing applications in Ti-indiffused waveguides, the combination of grating lenses and the Nb_2O_5 transition waveguide will allow us to obtain lens functions that have both high efficiency and large angular field of view (~4°).

I. Introduction

Chirped grating lenses on glass optical waveguides (Fig. 1) have been fabricated successfully with high throughout efficiency, several degrees angular field of view, and near diffraction-limited performance.[1,2] However, for some signal processing applications, such as the rf spectrum analyzer, it is necessary to fabricate grating lenses on $LiNbO_3$ waveguides. Recently, the theoretical design and fabrication of diffraction grating lenses on single-mode Ti-indiffused $LiNbO_3$ waveguides were reported.[3,4]

The experimentally measured performance of chirped grating lenses on Ti-indiffused waveguides indicates that it is difficult to get both high efficiency and more than two degrees of angular field of view for two reasons: (a) The mode index of Ti-indiffused $LiNbO_3$ n_e is close to the substrate index n_s. Therefore, the coupling of the energy to the substrate may limit the maximum angular field of view or the efficiency of small f/No. grating lenses.[5] (b) The Ti-indiffused $LiNbO_3$ waveguides have large mode depth (typically 1.5–2.5 μm). The large mode depth implies a small coupling coefficient, thus requiring long grating grooves which limit the angular field of view. To improve the grating lens performance, an alternative waveguide in $LiNbO_3$ other than Ti-indiffused is needed that has smaller mode depth and larger mode index. If Ti-indiffused $LiNbO_3$ must be used for other signal processing functions, such as acoustooptic interaction in the rf spectrum analyzer, the alternate waveguide may be used as a transition waveguide interconnecting two sections of Ti-indiffused regions for the grating lens fabrication as shown in Fig. 2.

II. Nb_2O_5 Interconnection Waveguides

The formation of lightguiding interconnections on glass waveguides was first demonstrated by Tien *et al.*[6] However, it was thought that such structures would result in a relatively high loss if used on $LiNbO_3$ substrates due to the surface roughness of commercially available $LiNbO_3$ crystals.[7] Since then, fabrication of very low loss (<0.5-dB/cm) Nb_2O_5 films on $LiNbO_3$ substrates has been reported.[8] As an alternative approach to improve the performance of chirped grating lenses on Ti-indiffused $LiNbO_3$, we have investigated the feasibility of such interconnections on $LiNbO_3$ substrates using Nb_2O_5 films. Figure 2 shows the cross section of a y-cut $LiNbO_3$ crystal with two Ti-indiffused guiding regions that have been connected by a Nb_2O_5 film. Since the refractive index of the Nb_2O_5 film (n = 2.24–2.28) is larger than the refractive index of the Ti-indiffused layers, a much larger angular field of view and smaller f/No. may be expected for grating lens structures fabricated on the Nb_2O_5 waveguides.

III. Nb_2O_5 Film Fabrication

The niobium pentoxide films were formed by reactively sputtering a high purity niobium metal target in an oxygen–argon atmosphere. This is a widely used technique for forming a variety of metal oxide waveguides and has resulted in Nb_2O_5 waveguides exhibiting high refractive index (n = 2.26 at Mortorola and n = 2.24 at UCSD at λ = 0.633 μm) and low optical loss. It should be noted that the optical properties of Nb_2O_5 waveguides have been found to be very sensitive to the conditions under which they are deposited[9] necessi-

Shih-Key Yao is with TRW Technology Research Center, 2525 East El Segundo Boulevard, El Segundo, California 90245; R. L. Davis is with Motorola, 8201 East McDowell Road, Scottsdale, Arizona 85257; the other authors are with University of California at San Diego, Department of Electrical Engineering & Computer Sciences, La Jolla, California 92093.

Received 13 May 1983.
0003-6935/83/193128-05$01.00/0.

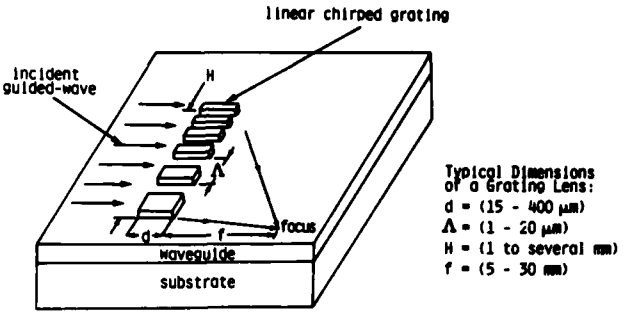

Fig. 1. Bragg diffraction chirped grating lens.

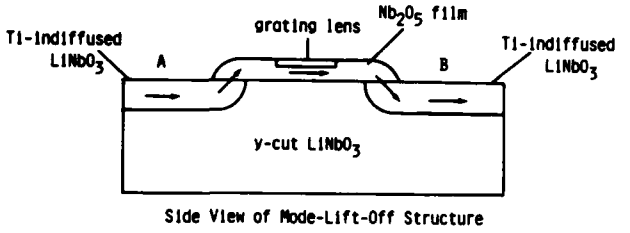

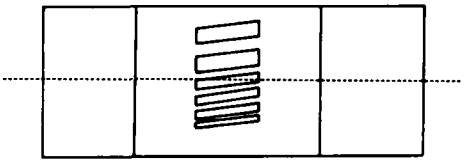

Fig. 2. Nb_2O_5 transition waveguide.

tating stringent control of the deposition environment to insure reproducible results. The Nb_2O_5 films at Motorola are deposited in rf diode system using a 15-cm diam × 0.5-cm thick MARZ grade niobium metal target. Both target and substrate platforms are water-cooled and separated by ~8 cm. After the sputtering chamber has been evacuated, the high vacuum pump is throttled down, and oxygen and argon are introduced through separate micrometer needle valves. The partial pressures of the gases are 1-mTorr O_2 and 3-mTorr Ar. Low chamber pressure during the process tends to result in better quality waveguides, but further reduction in the total pressure results in the inability to maintain a stable discharge at the rf power levels used. The depositions were made with 75 W (0.41 W/cm^2) of rf power. The cathode (target) assumed a bias potential of 720 V, and the substrate was allowed to float with respect to ground. As noted by Ingrey and Westwood,[10] the low power level is dictated by the relatively low melting temperature of the pentavalent oxide phase and film growth. The combination of low pressure and low power results in a deposition rate of ~750 Å/h. Films grown in these conditions exhibit no evidence of crystallinity under x-ray diffraction analysis. Prior to deposition, the $LiNbO_3$ substrates were prepared as follows. First, they were scrubbed with a detergent and rinsed. This rinse, as were all subsequent rinses, was done in high resistivity de-ionized water. Next they were placed in a room temperature stripping solution of chromic and sulfuric acids for 5–10 sec and rinsed. Then they were gently agitated in a detergent solution followed by a thorough rinsing. Finally, a succession of 30-sec baths in acetone, TCA, and acetone again was followed by a final rinsing. The substrates then were spun dry and immediately placed in the sputtering chamber; 5-cm (2-in.) diam oxidized silicon wafers were also placed in the chamber, and the films deposited on these wafers were analyzed for refractive index and optical loss. A qualitative assessment of these films indicated propagation losses of <1 dB/cm, which was subsequently confirmed by quantitative measurements of the films on the $LiNbO_3$ substrates. The film refractive index was determined by prism coupling 0.633-μm radiation from a He–Ne laser to the various waveguide modes and measuring the mode launch angles. The mode spectra were then fit to a step-index waveguide dispersion diagram. At Motorola, we measured a refractive index of 2.278 ± 0.005 for the films grown on the oxidized silicon substrates. The films on the $LiNbO_3$ substrates exhibited a refractive index of only 2.258 ± 0.005.

IV. Nb_2O_5 Taper Formation and Evaluation

An extensive amount of research has been carried out in controlling the profile of sputtered films for the fabrication of integrated optics devices such as Luneberg lenses.[11] Edges with long tapers and very gentle slopes can be obtained by undercutting the bottom surface of the shadowing masks. Milton *et al.*[12] have developed theories to calculate the optimum taper length for an adiabatic transition of power in branching waveguides that may be used to optimize taper performance. We have experimentally studied and evaluated several taper profiles using glass shadow masks during the sputtering process. Glass masks, instead of metal masks, are used to avoid perturbation of the electric field. Figure 3 shows the mask configuration used during the deposition process and the thickness variation of two transition waveguides measured by a Dektak. The insertion loss of tapered interconnections is measured by placing the input prism coupler on side *A* of the Ti-indiffused waveguide and the output prism on side *B* as illustrated in Fig. 2. The total insertion loss is the logarithm of the ratio of the power detected on side *B* to the power that would have been detected by the output coupler if the Ti-indiffused waveguide were continuous with no Nb_2O_5 interconnection. All the Ti-indiffused waveguides were evaluated before the deposition of interconnection regions. Without the interconnection waveguides, all guided-wave energy coupled into side *A* was lost to the substrate, and no guided energy was detected at the *B* side of the Ti-indiffused guides. Some of the measured results with the tapered interconnection Nb_2O_5 waveguide are listed in Table 1. The lowest insertion loss measured was 0.8 dB when the two sections of the Ti-indiffused waveguides were separated by 1 mm. The shadow mask used during the sputtering of Nb_2O_5 was 1 mm thick

Table I. Total Nb_2O_5 Waveguide Interconnection Loss and Taper Transition Slopes of Four of the Samples Made at UCSD and Motorola [a]

Distance between two Ti-indiffused regions (mm)	Nb_2O_5 interconnection length (mm)	Maximum taper slope (mrad)	Insertion loss (dB)
1.0	4.4	0.54	−0.8 (UCSD)
2.0	6.3	0.54	−1.4 (Motorola)
2.0	5.1	1.8	−2.5 (Motorola)
2.0	5.6	1.8	−7.0 (UCSD)

[a] Here the guided-wave mode is propagating in the x direction and is incident at an angle approximately perpendicular to the tapered edge of the Nb_2O_5 transition waveguide.

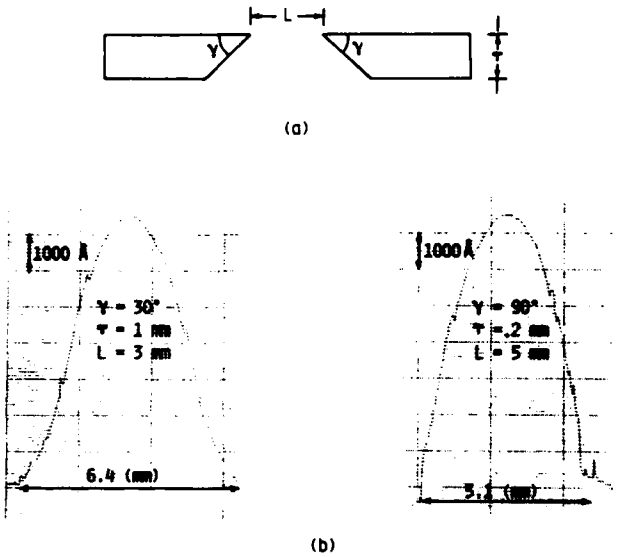

Fig. 3. (a) Configuration of the shadow mask during sputter deposition of Nb_2O_5 film; (b) thickness profile of a Nb_2O_5 transition waveguide measured by the Dektak.

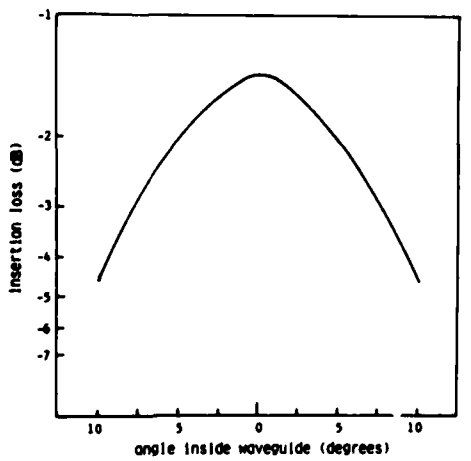

Fig. 4. Measured insertion loss of a Nb_2O_5 waveguide as a function of the angular deviation of the propagation direction with respect to the ordinary axis.

with the undercutting angle of 30°. However, the refractive index of the Nb_2O_5 film in the interconnection region is between the ordinary and extraordinary indices of the $LiNbO_3$ substrate. The propagation characteristics of any TE mode propagating in a direction α from the x axis may be approximated by an isotropic step-index waveguide that has a film index of 2.26 and substrate index of $(n_e^2 \cos^2\alpha + n_o^2 \sin^2\alpha)^{1/2}$, where n_e and n_o are the extraordinary and ordinary indices of $LiNbO_3$ crystal, respectively. The TE mode of such an isotropic step-index waveguide will be beyond cutoff at some values equal to α. Therefore, we would expect that the insertion loss of the interconnection to increase as the guided wave propagation direction deviates from the ordinary axis of the $LiNbO_3$ crystal, i.e., the axis. The increase of the insertion loss may also be partly due

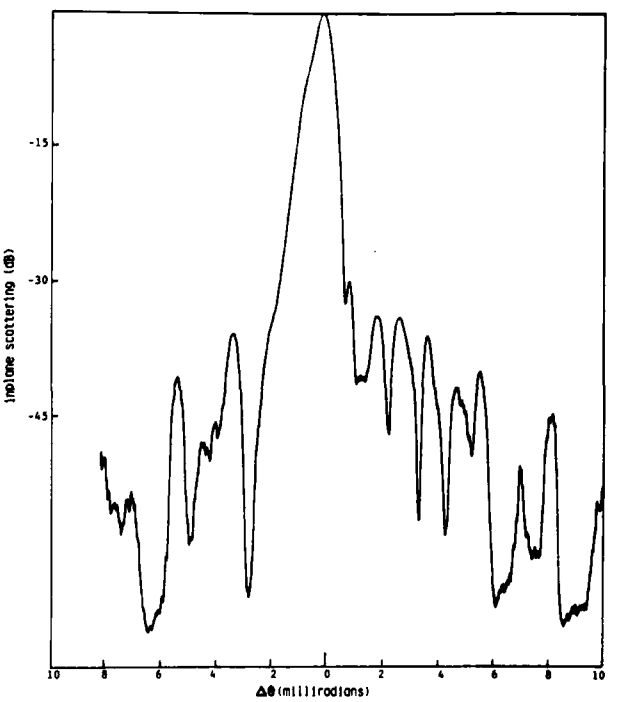

Fig. 5. In-plane scattering intensity of the guided-wave energy coupled out of a Ti-indiffused $LiNbO_3$ waveguide without interconnection waveguide.

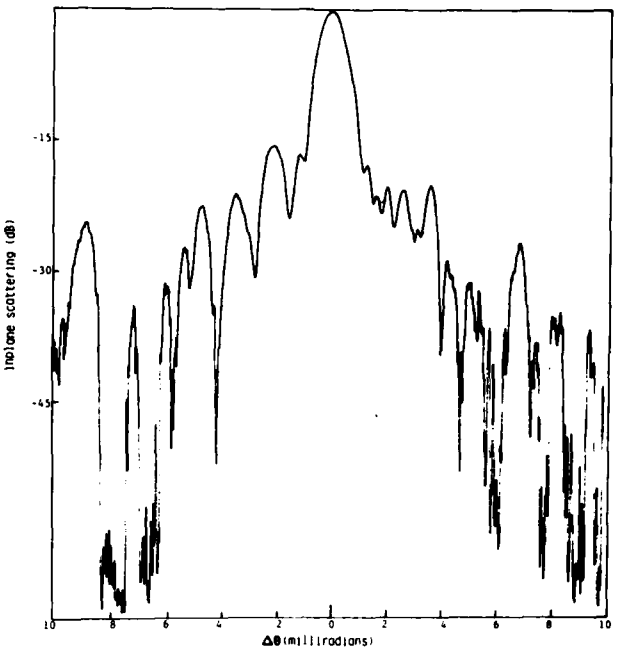

Fig. 6. In-plane scattering intensity of the guided-wave energy coupled out after passing through the Nb_2O_5 interconnection region.

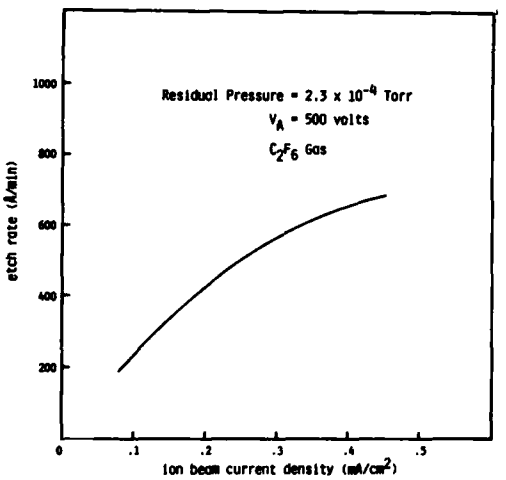

Fig. 7. Variation of etching rate of Nb_2O_5 film as a function of ion beam current density.

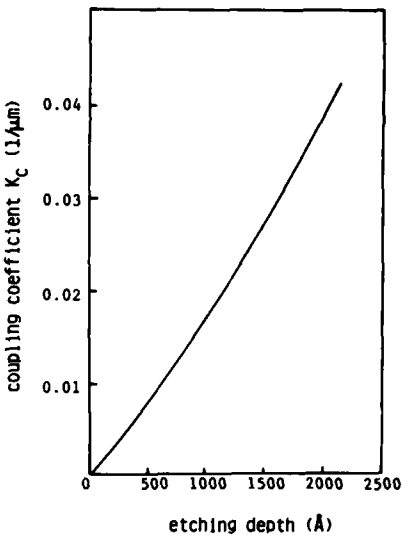

Fig. 8. Coupling coefficient vs etching depth of a Nb_2O_5 film with refractive index of 2.26 on $LiNbO_3$ substrate. The Nb_2O_5 film thickness of the waveguide is 7000 Å.

to the leaky mode for Ti-indiffused waveguide.[13] The measured insertion loss as a function of the angular deviation of the propagation direction with respect to the x axis is illustrated in Fig. 4. Larger indices of the Nb_2O_5 film in the interconnection region will reduce the dependence of the insertion loss on the angular deviation.

A parameter that may limit the usefulness of such interconnections for applications such as the rf spectrum analyzer is the amount of the in-plane scattering introduced by the taper edges. Figure 5 shows the angular spectrum of the guided-wave energy at $\lambda = 0.6328$ μm coupled out of a Ti-indiffused $LiNbO_3$ waveguide by a prism coupler without any interconnection waveguide. The guided-wave energy is excited by an input prism coupler using a He–Ne laser. Thus the measured in-plane scattering includes that of the prism couplers. Figure 6 shows the angular spectrum of the guided-wave energy coupled out after passing through the Nb_2O_5 interconnection region. The same prism couplers were

used for both measurements. As seen from the two figures, an addition of 10–15 dB of scattered noise has been introduced due to the Nb_2O_5 transition. However, since no special care had been undertaken to minimize the amount of the scattering loss in our tapered connection, we believe that a much lower scattering loss can be achieved when the taper slopes and lengths are optimized.

V. Grating Lens Fabrication on Nb_2O_5 Waveguides

Experimentally, we have investigated different processes for the fabrication of the chirped grating grooves on Nb_2O_5–$LiNbO_3$ waveguides that will yield large coupling coefficient values. The fabrication of TiO_2 grating grooves[14] on Nb_2O_5 films failed because the Nb_2O_5 refractive index and loss dramatically changed after the Ti-oxidation process at 450°C. Thus the grating grooves must be fabricated by etching. The reactive ion beam etch (RIBE) technique using Freon gas was employed to etch the grating grooves in the Nb_2O_5 film. Variation of the Nb_2O_5 etching rate as a function of the ion beam current density is illustrated in Fig. 7. We have etched up to 4000 Å of Nb_2O_5 film with good pattern resolution of the grating grooves using Shipley AZ 1350 photoresist masks. Figure 8 shows the calculated coupling coefficient as a function of the groove depth on the Nb_2O_5 waveguide. Clearly, fairly large K_c can be expected with a moderate depth of etching. We have fabricated several lenses on Nb_2O_5–$LiNbO_3$ waveguides. The specifications of the mask pattern used are: $\Lambda_{min} = 1.73\ \mu m$; $\Lambda_{max} = 3.45\ \mu m$; focal length ($f$) $\simeq$ 12 mm; grating groove length $d = 40\ \mu m$; lens width (h) = 1 mm; and f/No. $\simeq$12. The highest throughput efficiency measured for the above lens was 85 ± 5% for the groove depth of $\simeq$2000 Å. The efficiency measurements were made by prism couplers. The throughput efficiency is the ratio of power measured in the diffracted beam focused at the focal point to the power measured in the guided-wave beam transmitted through the waveguide when the transverse location of the incident beam is moved to bypass the lens. The diffraction efficiency is the ratio of the power measured in the focused beam to the sum of the powers measured in all the orders of diffraction. For the lenses fabricated on Nb_2O_5 films, the diffraction efficiency was equal to the throughput efficiency, implying that very little power was converted by the lens to the substrate modes. The measured angular field of view for the lens was $\Delta\theta \simeq 4°$. The angular field of view $\Delta\theta$ is the change in the incidence angle, within which the measured efficiency is larger than one half of the highest efficiency.

VI. Conclusions

The feasibility of using a Nb_2O_5 transition waveguide to interconnect two separate sections of Ti-indiffused waveguide has been demonstrated with a total insertion loss of 0.8 dB. The key to the low loss transition is a very smooth taper obtained by sputtering using a glass shadow mask. Nb_2O_5 waveguides obtained by reactive sputtering of Nb in an O_2–Ar atmosphere has a propagation loss of <1 dB/cm in the x or y direction. The chirped grating lens fabricated on top of such a waveguide by reactive ion beam etching has an 85% throughput efficiency and four degrees of angular field of view. Thus the combination of the tapered transition waveguide and the grating lens will allow us to obtain the lens function with high efficiency and large angular field of view for any signal processing applications using Ti-indiffused $LiNbO_3$ without the disadvantage of the deep mode depth and small $n_e - n_s$ value. Such a technique may also be used to modify the mode profile of Ti-indiffused waveguides in other applications such as butt coupling, directional coupling, or switching. It has two drawbacks: (1) The propagation loss increases as the direction of propagation is moved away from the x or y axes because the ordinary index of $LiNbO_3$ is larger than the index of the Nb_2O_5 film. (2) The Nb_2O_5 waveguide will be affected severely by any subsequent processing that has a temperature higher than 400°C.

This work is supported in part by AFOSR grant 80-0037 with the University of California, San Diego. R. L. Davis is now at Northrop Research and Technology Center, Rolling Hills Estate, California 90274.

References

1. J.-M. Delavaux, S. Forouhar, W. S. C. Chang, and R.-X. Lu, in *Technical Digest, Conference on Lasers and Electrooptics* (Optical Society of America, Washington, D.C., 1982), paper TH06.
2. S. K. Yao and D. E. Thompson, Appl. Phys. Lett. **33,** 635 (1978).
3. Z.-Q. Lin, S.-T. Zhou, W. S. C. Chang, S. Forouhar, and J.-M. Delavaux, IEEE Trans. Microwave Theory Tech. **MTT-29,** 881 (1981).
4. W. S. C. Chang, S. Forouhar, J.-M. Delavaux, and R.-X. Lu, "Chirped Grating Lenses in Ti-indiffused $LiNbO_3$ Optical Waveguides," in *Proceedings, European Conference on Optical Systems and Applications, Edinburgh, Scotland, 7–10 Sept. 1982,* to be published.
5. S. K. Yao, Proc. Soc. Photo-Opt. Instrum. Eng. **269** (Feb. 1981).
6. P. K. Tien, R. J. Martin, and G. Smolinsky, Appl. Opt. **12,** 1909 (1973).
7. H. P. Hsu and A. F. Milton, IEEE J. Quantum Electron. **QE-13,** 224 (1975).
8. R. L. Davis, "RF Sputtered Thin Film Niobium Pentoxide for Intetgrated Optics," at American Vacuum Society Symposium, Scottsdale, Ariz. (Feb. 1982).
9. R. L. Davis and F. S. Hickernell, "Thin Film Oxides of Vanadium, Niobium, and Tantalum for Integrated Optics," at SPIE Technical Symposium East, Washington, D.C., (Apr. 1983).
10. S. J. Ingrey and W. D. Westwood, Appl. Opt. **15,** 607 (1976).
11. S. K. Yao, D. B. Anderson, C. M. Oaria, and V. G. Kreismanis, in *Technical Digest, Topical Meeting on Integrated and Guided Wave Optics* (Optical Society of America, Washington, D.C., 1977),
12. A. F. Milton and W. K. Burns, Appl. Opt. **14,** 1207 (1975).
13. W. A. Burns, S. K. Sheem, and A. F. Milton, IEEE J. Quantum Electron **QE-15,** 1282 (1979).
14. S. Forouhar, C. Warren, R.-X. Lu, and W. S. C. Chang, "Techniques for the Fabrication of High-Index Overlay Films on $LiNbO_3$," at SPIE Technical Symposium, Arlington, Va. (Apr. 1983).